Earth and Planetary Science Letters, 97 (1990) 353–368
Elsevier Science Publishers B.V., Amsterdam – Printed in The Netherlands

[MK]

Evolution of Atlantic–Pacific $\delta^{13}C$ gradients over the last 2.5 m.y.

M.E. Raymo [1]*, W.F. Ruddiman [1], N.J. Shackleton [2] and D.W. Oppo [1]**

[1] *Lamont-Doherty Geological Observatory, Palisades, NY 10964 (U.S.A.)*
[2] *Subdepartment of Quaternary Research, Godwin Laboratory, Free School Lane, Cambridge, CB2 3RS (U.K.)*

Received July 7, 1989; accepted after revision December 8, 1989

The evolution of interocean carbon isotopic gradients over the last 2.5 m.y. is examined using high-resolution $\delta^{13}C$ records from deep sea cores in the Atlantic and Pacific Oceans. Over much of the Northern Hemisphere ice ages, relative reductions in North Atlantic Deep Water production occur during ice maxima. From 2.5 to 1.5 Ma, glacial reductions in NADW are less than those observed in the late Pleistocene. Glacial suppression of NADW intensified after 1.5 Ma, earlier than the transition to larger ice sheets around 0.7 Ma. At a number of times during the Pleistocene, $\delta^{13}C$ values at DSDP Site 607 in the North Atlantic were indistinguishable from eastern equatorial Pacific $\delta^{13}C$ values from approximately the same depth (ODP Site 677), indicating significant incursions of low $\delta^{13}C$ water into the deep North Atlantic. Atlantic/Pacific $\delta^{13}C$ values converge during glaciations between ~1.13–1.05 m.y., 0.83–0.70 m.y., and 0.46–0.43 m.y. This represents a pseudo-periodicity of approximately 300 kyr which cannot easily be ascribed to global ice volume or orbital forcing. This partial decoupling, at low frequencies, of the $\delta^{18}O$ and $\delta^{13}C$ signals at Site 607 indicates that variations in North Atlantic deep water circulation cannot be viewed simply as a linear response to ice sheet forcing.

1. Introduction

The deep waters of the world's oceans are formed by the cooling and sinking of surface waters at high latitudes. Today, the high-latitude North Atlantic is a major area of bottom water formation. Here, dense North Atlantic Deep Water (NADW) is produced by intense evaporative cooling of the warm, saline waters advected northward by the Gulf Stream [1]. The resulting thermohaline overturn, in the Labrador and Norwegian–Greenland Seas, then perpetuates the deep water formation process by drawing additional warm thermocline water northward. Because NADW formation plays a vital role both in the ventilation of the world's deep oceans (through the introduction of oxygen) and in the modulation of local climate (through the release of evaporative heat), we might expect that variations in NADW production would have significant consequences both in the deep sea and on the Earth's surface. In addition, variations in NADW may be an important factor controlling glacial–interglacial changes in atmospheric CO_2 [2–4]. In this paper, we use carbon isotopic records to reconstruct the history of NADW production since the late Pliocene.

$\delta^{13}C$ is a useful tracer of paleoceanographic changes in deep water circulation (see Curry et al. [5] for an extensive review). NADW, which is formed with an initial $\delta^{13}C$ value between 1.0 and 1.5‰, becomes gradually lower in $\delta^{13}C$ as it travels southward and mixes with Southern Ocean Water (SOW), which has an average $\delta^{13}C$ value of 0.3‰ [6]. As this deep water travels to the Pacific Ocean, its $\delta^{13}C$ is further reduced by ~0.5‰ by aging [6]. This effect, driven by the continuous oxidation of low-$\delta^{13}C$ organic matter falling from the surface, gradually causes the carbon isotopic value of deep waters to become even more negative (aging effects are relatively unimportant in the Atlantic Ocean due to the short residence time of deep waters in this basin; < 100 years [7]). By reconstructing deep water $\delta^{13}C$ patterns in the past, paleoceanographers can determine the path of deep water flow (aging) and the strength of

Present addresses:
* Department of Geology, Melbourne University, Parkville, Vic. 3052 (Australia).
** Woods Hole Oceanographic Institution, Woods Hole, MA 02543 (U.S.A.).

0012-821X/90/$03.50

mixing between different source components of deep water.

In addition to $\delta^{13}C$ variations caused by the aging and mixing of water masses, $\delta^{13}C$ variations due to changes in the amount of organic carbon sequestered on continents and shelves must also be considered [8]. Because organic matter $\delta^{13}C$ values range from -21 to $-25‰$ [9], any alteration in the size of this reservoir will cause oceanic $\delta^{13}C$ values to change. Duplessy et al. [10] estimate that an increase in continental biomass since the last glaciation has resulted in a 0.32‰ rise in the average carbon isotopic composition of the ocean. However, because this change is imbedded within all oceanic $\delta^{13}C$ records equally, it does not affect $\delta^{13}C$ *gradients* within the ocean.

The Wisconsin–Holocene glacial–interglacial (G–I) transition was characterized by a large-scale reorganization of deep-water circulation patterns. Boyle and Keigwin [11], Curry and Lohmann [12], and Shackleton et al. [13], among others, have used the distinctive $\delta^{13}C$ signatures of deep Atlantic and deep Pacific waters, recorded in deep-sea benthic foraminifera, to show that relatively less NADW was formed during the last glacial maximum. The deep Atlantic basin, which is now dominated by NADW, appears to have contained significantly more nutrient-enriched, ^{13}C-depleted waters of Antarctic and Pacific origin.

This was confirmed by Oppo and Fairbanks [14] who, using continuous $\delta^{13}C$ records, traced the migration of the mixing front between northern and southern source deep water over the last 20,000 years in the Atlantic basin. At the last glacial maximum, the mixing zone between high-$\delta^{13}C$ NADW and low-$\delta^{13}C$ SOW (formed by a mixture of AABW and recirculated Pacific water) migrated northward, indicating relatively weaker influence of NADW in the deep Atlantic. By using $\delta^{13}C$ records near each of the areas of deep water formation, Oppo and Fairbanks were able to determine uniquely what fraction of the $\delta^{13}C$ signal observed in the mixing zone was due to actual circulation changes and what fraction was due to glacial–interglacial transfers between ^{13}C reservoirs which affect all areas of the ocean equally.

In this paper we use this method to address three questions: (1) How have Atlantic–Pacific $\delta^{13}C$ gradients, and thus the relative strength of NADW production, varied through time? (2) To what extent are variations in deep ocean circulation and global ice volume related? and (3) What factors drive variations in deep water circulation? High-resolution paleoceanographic studies of Atlantic–Pacific $\delta^{13}C$ gradients, a measure of the relative production and export of ^{13}C-enriched NADW to the ^{13}C-poor Pacific Ocean, previously extended back to 0.215 m.y. BP [11]. Here, we present $\delta^{13}C$ records from the Atlantic and Pacific Oceans which extend to 2.5 m.y. BP, the time of Northern Hemisphere ice age initiation.

2. Core selection and analysis

Isotopic records are presented from three sites: DSDP Sites 552 (56° N 23° W) and 607 (41° N 33° W), and ODP Site 677 (1° N 84° W). Site 552 is located closest to the area of modern NADW production (Fig. 1). This water mass is formed by a combination of three different water types, Labrador Sea Water (LSW), Denmark Strait Overflow Water (DSOW), and Gibbs Fracture Zone Water (GFZW), which mix and flow southward at a core depth of ~ 3400 m. GFZW, volumetrically the most important component of NADW, consists of Norwegian Sea Overflow Water (NSOW) which entrains significant amounts of both LSW and Mediterranean Overflow Water (MOW) at depths of 1000–2000 m after exiting the Norwegian and Greenland Seas. This water then passes through the Gibbs Fracture Zone and mixes with DSOW before turning south.

Site 552, recovered from the southwestern flank of the Rockall Plateau at 2301 m, lies in the path of this overflow today. At the last glacial maximum, $\delta^{13}C$ values at this site were lower by ~ 0.32‰. Because this difference is equivalent to the estimated mean ocean glacial–interglacial $\delta^{13}C$ signal [10], we can infer that a water mass similar to modern GFZW bathed this site at 18 kyr BP [15].

Site 607, recovered on the western flank of the Mid-Atlantic Ridge at 3427 m and located at the core depth of NADW today, is ideally situated to measure the relative strength of NADW versus SOW in the deep North Atlantic. As NADW moves southward and mixes with SOW it becomes progressively lower in $\delta^{13}C$. The ~ 0.6‰ increase

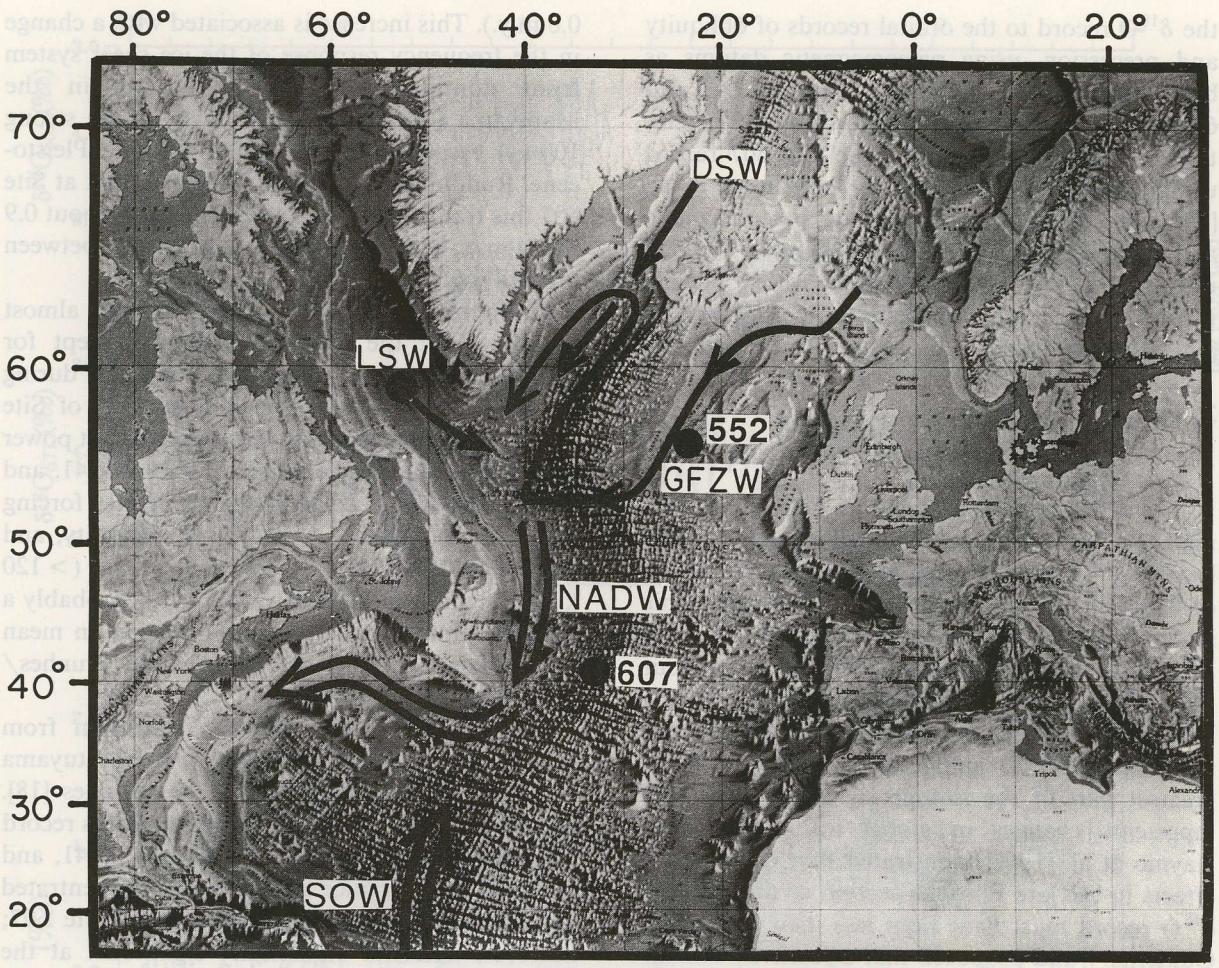

Fig. 1. Map of North Atlantic showing paths followed by major deep water masses; including Labrador Sea Water (*LSW*), Denmark Strait Water (*DSW*), Gibbs Fracture Zone Water (*GFZW*), North Atlantic Deep Water (*NADW*), and Southern Ocean Water (*SOW*). Site 552 and 607 core locations are also indicated.

in $\delta^{13}C$ observed for the last G–I transition at this site indicates that, in addition to the 0.32‰ global mean-ocean $\delta^{13}C$ change, an increase in the strength of NADW production [e.g. 11] caused a ~ 0.3‰ $\delta^{13}C$ increase at this site.

Site 677, located in the eastern equatorial Pacific at 3461 m (approximately the same depth as Site 607) is used to measure deep Pacific–Atlantic $\delta^{13}C$ fractionation through time. As noted previously [11], the Pacific–Atlantic $\delta^{13}C$ difference provides a measure of the relative strength of NADW export from the North Atlantic. Similarly, the $\delta^{13}C$ difference between Sites 607 and 552 is also a measure of the relative strength of NADW production, with a larger difference at times when relatively little high-$\delta^{13}C$ northern component water reaches the deep North Atlantic.

The $\delta^{18}O$ and $\delta^{13}C$ data presented in this paper have all been corrected for species offsets using the corrections of Shackleton and Hall [16]. The Site 607 and 552 isotopic records are based primarily on the analysis of *Cibicidoides*; the Site 607 data are published in Ruddiman et al. [17] and Raymo et al. [15], and the Site 552 data in Shackleton and Hall [16]. The 677 data is based primarily on analysis of *Uvigerina* and is published in Shackleton and Hall [18]. Average sampling intervals at Sites 552, 607, and 677 are 7.0, 3.4, and 2.9 kyr, respectively.

The Site 607 time scale was generated by tuning

the $\delta^{18}O$ record to the orbital records of obliquity and precession, using paleomagnetic datums as basic time constraints [15,17]. The Site 552 and 677 time scales were generated by graphic correlation of their $\delta^{18}O$ signals to the Site 607 record using techniques developed by Martinson et al. [19] and constraints provided by paleomagnetic and biostratigraphic datums. Gaps in the Site 552 record represent sections not recovered or disturbed during the hydraulic piston coring process [15]. All data available by request to first author.

3. Results

3.1. Oxygen isotopes

The $\delta^{18}O$ records depicted in Figs. 2a and 3a mainly reflect variations in global ice volume with heavier $\delta^{18}O$ values caused by the glacial build-up of ^{16}O-enriched ice sheets on the continents. This is evidenced by the contemporaneous influxes of IRD into the North Atlantic Ocean throughout the 2.5 m.y. length of these records [20,21]. In the late Quaternary, temperature effects account for some of the $\delta^{18}O$ amplitude ($\sim 0.6‰$), but the greatest part of the isotope signal ($\sim 1.2–1.5‰$) represents changes in global ice volume [22]. Raymo et al. [15] demonstrated that temperature effects in the late Pliocene section of the Site 607 $\delta^{18}O$ record must have been less than in the late Quaternary and proposed that a relatively similar fraction of the $\delta^{18}O$ signal ($\sim 1/3$) was due to changes in temperature.

The most noticeable feature of Fig. 2a, given the variation in sampling intervals among these sites and the fact that they were run in different labs, is the similarity of all three $\delta^{18}O$ records over the entire 2.5 m.y. span of the ice ages. The amplitude modulation of the $\delta^{18}O$ record is generally in excellent agreement between these three cores. The only interval of significant amplitude mismatch, between 2.4 and 2.3 m.y., has been shown to be due to species effects in the Site 552 record. Curry and Miller [23] reanalyzed this section of Site 552 using only *Cibicidoides* and showed that the amplitude of the $\delta^{18}O$ signal within this interval reached values similar to Sites 607 and 677. Curiously, the $\delta^{13}C$ record did not appear to be affected by the species analyzed.

An increase in $\delta^{18}O$ amplitudes is observed in all three records during the Brunhes Chron (0.73–0.0 m.y.). This increase is associated with a change in the frequency response of the ice sheet system from dominantly 41-kyr variations in the Matuyama Chron (2.47–0.73 m.y.), to the strong 100-kyr response which typifies the late Pleistocene. Ruddiman et al. [17] have shown that at Site 607 this transition occurs gradually from about 0.9 to 0.4 m.y., with the fastest rate of change between 0.7 and 0.6 Ma.

Prior to 0.9 Ma, $\delta^{18}O$ variations occur almost exclusively at the 41-kyr frequency, except for transient increases in 100 and 23 kyr power during the latest Pliocene [15]. Spectral analysis of Site 607 (2.5–0.0 m.y.; Fig. 4a) shows significant power (at the 95% confidence interval) at 19, 23, 41, and 96 kyr, the major components of orbital forcing driven by variations in precession, obliquity, and eccentricity [24]. At very low frequencies (> 120 kyr), a significant peak at ~ 700 kyr is probably a manifestation of nonstationarity (change in mean and variance of $\delta^{18}O$ record) over the Brunhes/Matuyama transition [17,25].

Site 677 $\delta^{18}O$ also shows a transition from predominantly 41-kyr variation in the Matuyama to mostly 100-kyr variation in the Brunhes [18]. Spectral analysis of the entire length of this record (Fig. 4a) exhibits significant peaks at 23, 41, and 96 kyr. More variance appears to be concentrated around 400 kyr than was observed at Site 607; however, it is not statistically significant at the 95% level. Spectral analysis of Site 552 was not attempted due to a large sampling gap in this record (Fig. 2).

Plotted in Figs. 5a and b are orbital eccentricity [24] and a stack of the $\delta^{18}O$ records from Sites 552, 607, and 677. Oxygen isotope stage assignments are from SPECMAP [26] for the Brunhes, from Ruddiman et al. [17] for the early Pleistocene, and from Raymo et al. [15] for the late Pliocene. The stack was generated by interpolating all three records at 3.4-kyr intervals and averaging them together, excluding intervals of unrecovered sediment. Times of greater than average ice volume fall at intervals of 375–550 kyr (Fig. 5b). Spectral analysis of the $\delta^{18}O$ stack (Fig. 4b) shows significant peaks at 415–555, 96, 41, and 23 kyr. While there is obviously an important low-frequency component in the $\delta^{18}O$ stack, no straightforward correlation is observed with orbital eccentricity (Fig. 5a).

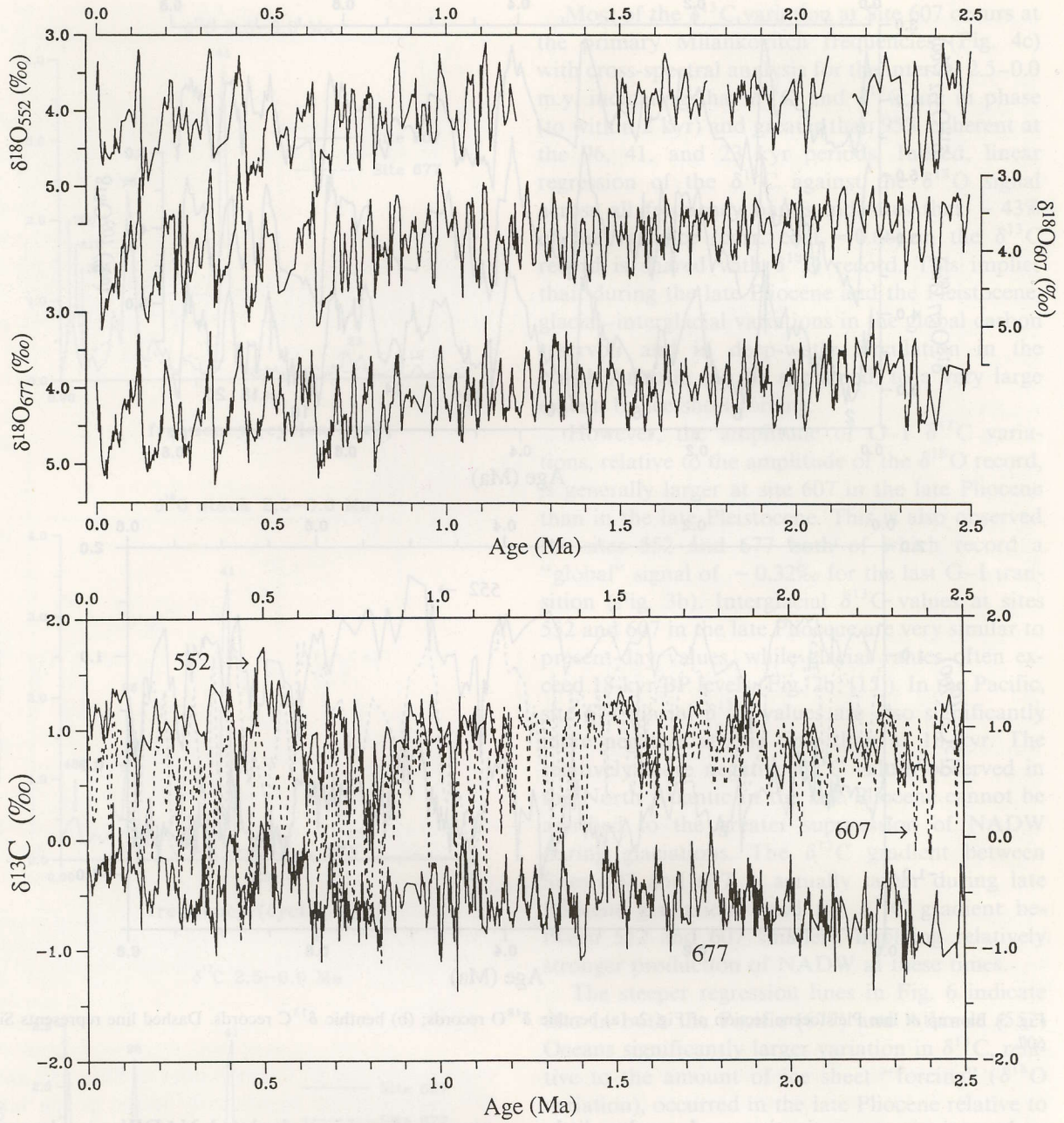

Fig. 2. (a) Variations in benthic $\delta^{18}O$ from DSDP Site 552, DSDP Site 607, and ODP Site 677 plotted to age; (b) benthic $\delta^{13}C$ records from same three sites corrected for species offsets (after Shackleton and Hall [16]). *Cibicidoides wuellerstorfi* was the primary species analyzed at Sites 552 and 607 while *Uvigerina perigrina* was the primary species analyzed at Site 677.

Because the time scale for 607, and by correlation for 552 and 677, was generated by tuning to obliquity and precession, concentration of variance at the 41, 23, and 19 kyr periodicities may be expected. However, these are dominant frequencies of variation even in the untuned records (see [15,17,26] for detailed discussion and evaluation of tuning process). Further, the use of a tuned time

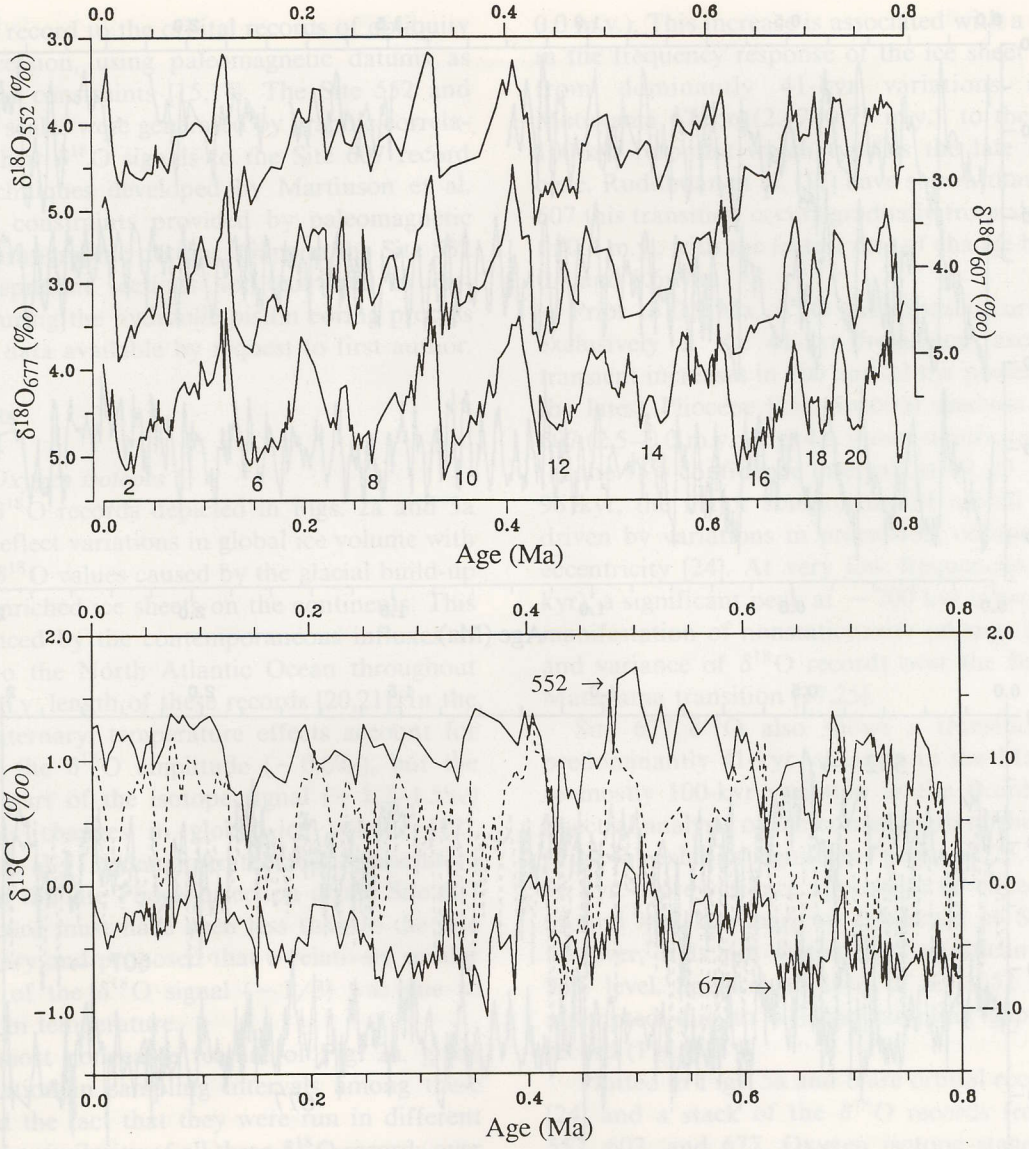

Fig. 3. Blowup of late Pleistocene section of Fig. 2: (a) benthic $\delta^{18}O$ records; (b) benthic $\delta^{13}C$ records. Dashed line represents Site 607.

scale versus a magnetic time scale makes little difference with respect to the long-term trends identified in the isotopic records.

3.2. Carbon isotopes

Figures 2b and 3b depict the evolution of $\delta^{13}C$ for the Pacific and Atlantic Oceans over the last 2.5 m.y. The fact that $\delta^{13}C$ values at Site 552 are always more positive than Pacific values (Site 677) indicates that the North Atlantic was always a source of nutrient-depleted NADW, an observation originally made by Shackleton et al. [20]. At Site 607, the pattern of $\delta^{13}C$ reduction at times of ice maxima (defined by times of more positive $\delta^{18}O$) is observed throughout the 2.4 m.y. length of the Northern Hemisphere ice age. In addition, the transition from a dominant 41-kyr response in the Matuyama to a mostly 100-kyr response in the Brunhes is observed in both the $\delta^{13}C$ and $\delta^{18}O$ records [17].

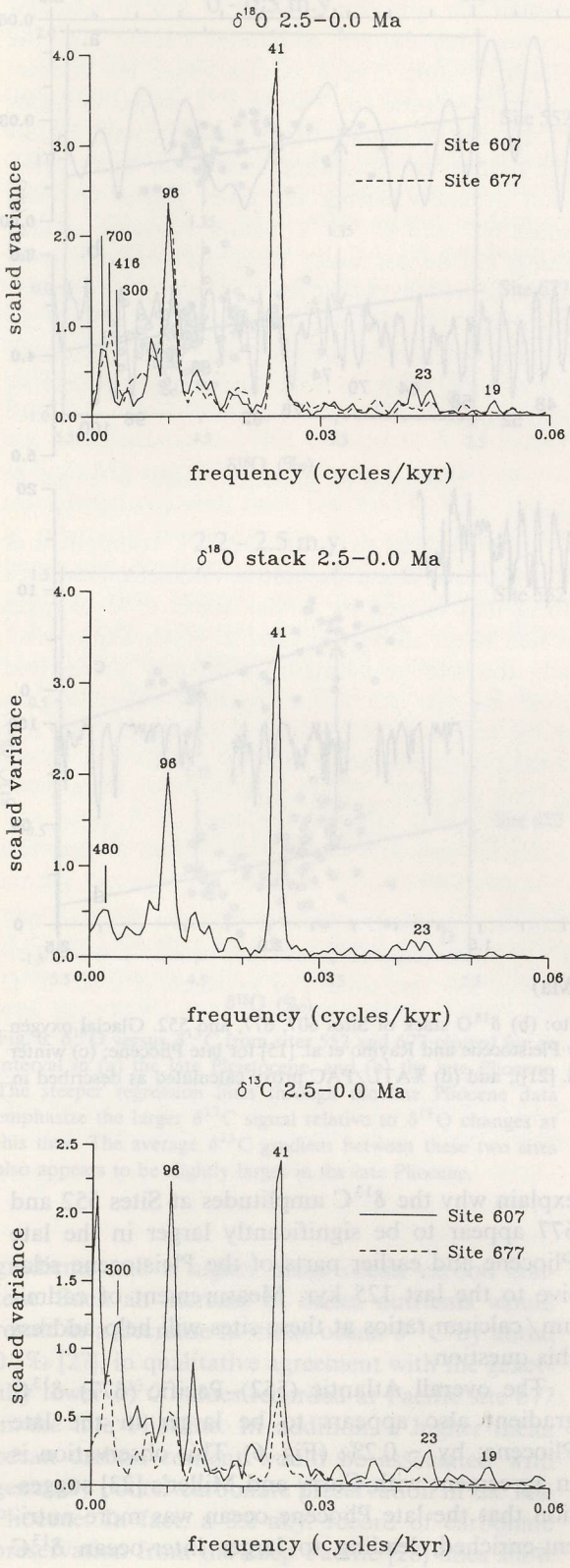

Most of the $\delta^{13}C$ variation at Site 607 occurs at the primary Milankovitch frequencies (Fig. 4c) with cross-spectral analysis for the interval 2.5–0.0 m.y. indicating that $\delta^{18}O$ and $\delta^{13}C$ are in phase (to within 2 kyr) and greater than 95% coherent at the 96, 41, and 23 kyr periods. Indeed, linear regression of the $\delta^{13}C$ against the $\delta^{18}O$ signal across all frequency bands indicates that ~ 43% of the variance (corr. coef. = 0.66) in the $\delta^{13}C$ record is shared with $\delta^{18}O$ record. This implies that, during the late Pliocene and the Pleistocene, glacial–interglacial variations in the global carbon reservoir and in deep-water circulation in the North Atlantic can be explained, to a very large extent, by ice sheet forcing.

However, the amplitude of G–I $\delta^{13}C$ variations, relative to the amplitude of the $\delta^{18}O$ record, is generally larger at site 607 in the late Pliocene than in the late Pleistocene. This is also observed for sites 552 and 677 both of which record a "global" signal of ~ 0.32‰ for the last G–I transition (Fig. 3b). Interglacial $\delta^{13}C$ values at sites 552 and 607 in the late Pliocene are very similar to present-day values, while glacial values often exceed 18-kyr BP levels (Fig. 2b; [15]). In the Pacific, site 677 glacial $\delta^{13}C$ values are also significantly more negative at this time than at 18 kyr. The relatively more negative $\delta^{13}C$ values observed in the North Atlantic in the late Pliocene cannot be ascribed to the greater suppression of NADW during glaciations. The $\delta^{13}C$ gradient between Sites 607 and 677 is actually larger during late Pliocene glaciations (and the $\delta^{13}C$ gradient between 552 and 607 smaller), implying relatively stronger production of NADW at these times.

The steeper regression lines in Fig. 6 indicate that in both the Pacific (677) and Atlantic (552) Oceans significantly larger variation in $\delta^{13}C$, relative to the amount of ice sheet "forcing" ($\delta^{18}O$ variation), occurred in the late Pliocene relative to

Fig. 4. All spectral analyses generated using Blackman–Tukey method with 1/3 lag; band-width in all cases equals 0.002. Unless noted, labelled peaks are significant at 95% confidence interval. (a) Site 607 and 677 $\delta^{18}O$ spectra; 416 kyr peak at Site 677 is not significant at 95%. No appreciable variance falls near 300 kyr at Site 607. (b) Spectra of $\delta^{18}O$ stack (generated as described in text). (c) $\delta^{13}C$ spectra from Sites 607 and 677. Unlike the $\delta^{18}O$ record, variance is observed at 300 kyr at Site 607; this peak is significant at 85% confidence interval.

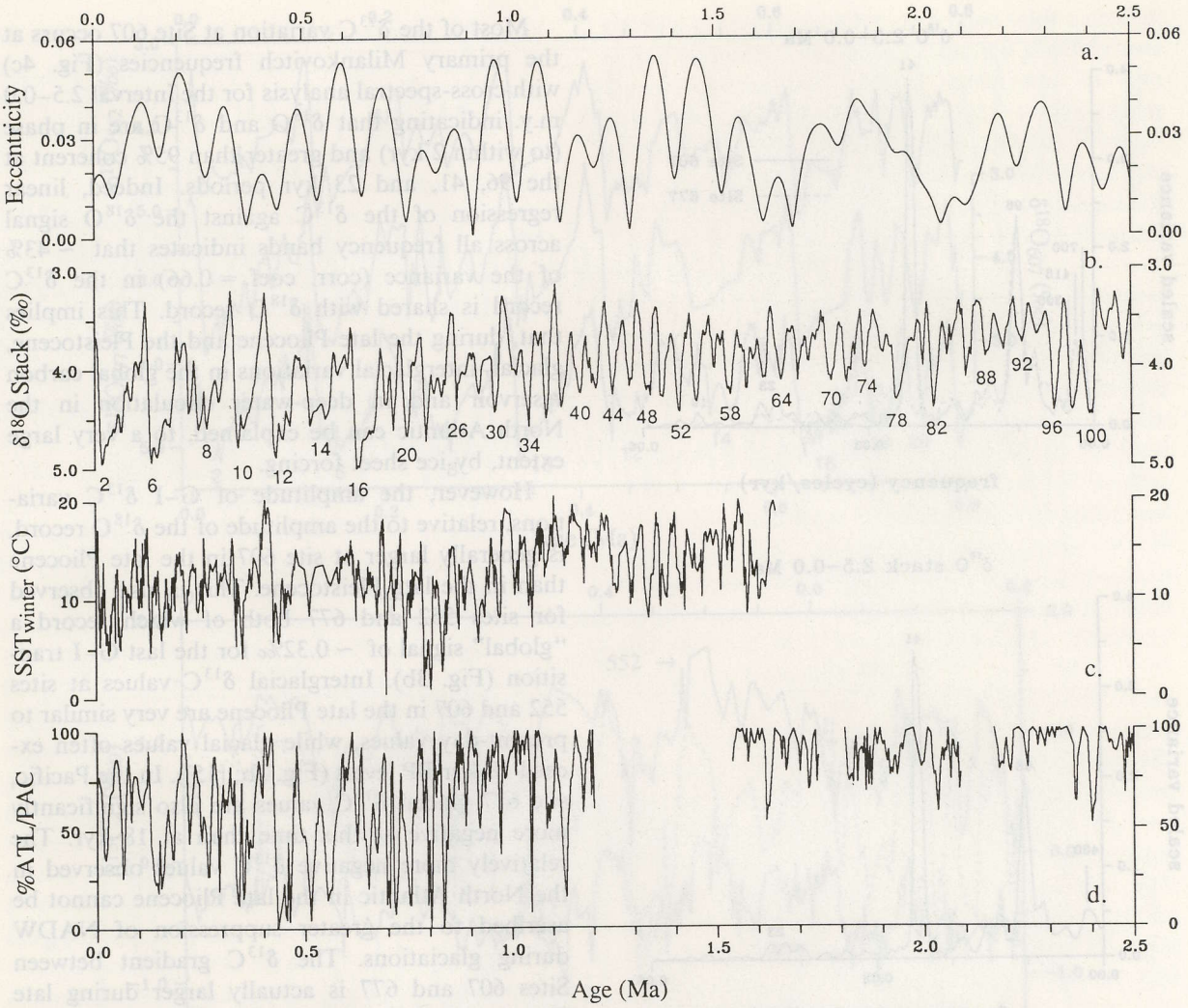

Fig. 5. (a) Orbital eccentricity variations over last 2.5 m.y. compared to: (b) $\delta^{18}O$ stack of Sites 607, 677, and 552. Glacial oxygen isotope stages are identified according to Ruddiman et al. [17] for early Pleistocene and Raymo et al. [15] for late Pliocene; (c) winter sea surface temperature estimates from Site 607 (after Ruddiman et al. [21]); and (d) %ATL/PAC proxy calculated as described in text.

the late Quaternary. The fact that both these sites vary with an approximate amplitude of 0.5–0.8‰ prior to 1.6 Ma may indicate that glacial–interglacial carbon transfers between oceanic and continental reservoirs were larger in the late Pliocene, resulting in mean oceanic G–I $\delta^{13}C$ changes of ~ 0.7‰ (versus 0.32‰ over the last glacial cycle [10]). Intuitively, this seems unlikely given that variations in ice sheets, and hence sea-level and climate, were reduced. Alternatively, circulation changes, including changes in preformed nutrient levels in areas of deep-water formation, could explain why the $\delta^{13}C$ amplitudes at Sites 552 and 677 appear to be significantly larger in the late Pliocene and earlier parts of the Pleistocene relative to the last 125 kyr. Measurement of cadmium/calcium ratios at these sites will help address this question.

The overall Atlantic (552)–Pacific (677) $\delta^{13}C$ gradient also appears to be larger in the late Pliocene; by ~ 0.2‰ (Fig. 6). This observation is in agreement with Curry and Miller's [23] suggestion that the late Pliocene ocean was more nutrient-enriched, leading to larger inter-ocean $\delta^{13}C$

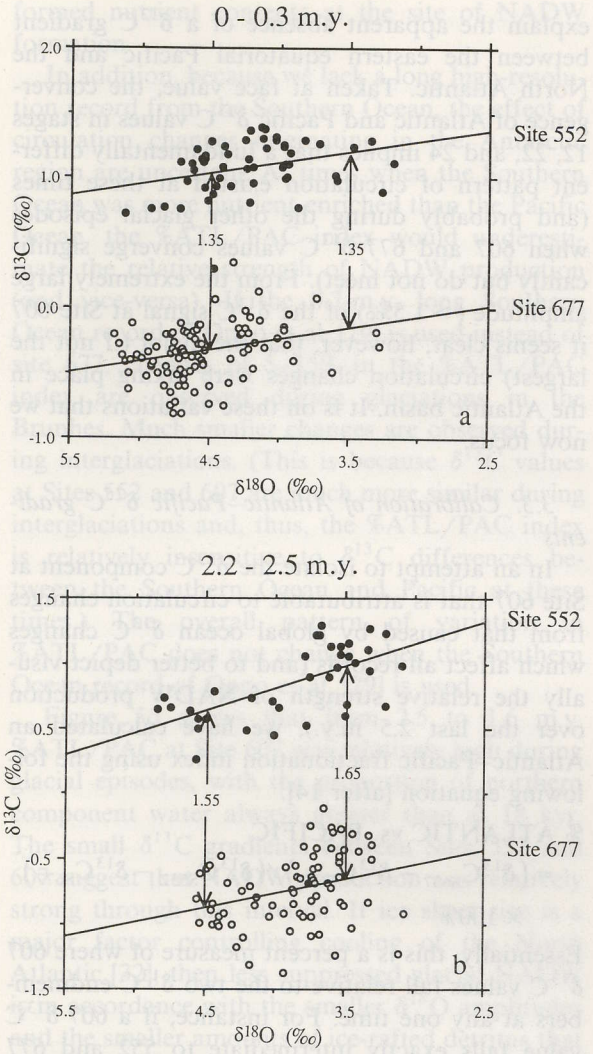

Fig. 6. $\delta^{18}O$ versus $\delta^{13}C$ from sites 552 and 677 plotted for an interval in (a) the late Pleistocene, and (b) the late Pliocene. The steeper regression lines through the late Pliocene data emphasize the larger $\delta^{13}C$ signal relative to $\delta^{18}O$ changes at this time. The average $\delta^{13}C$ gradient between these two sites also appears to be slightly larger in the late Pliocene.

gradients and a higher mean ocean carbon content. Such an increase in ocean nutrients would result in a decrease in mean ocean $\delta^{13}C$ by about 0.5‰ [27], in qualitative agreement with the generally lower $\delta^{13}C$ values recorded at Pacific site 677 in the late Pliocene. In addition, a higher mean ocean carbon content would be associated with generally poorer carbonate preservation in the late Pliocene. In fact, a 3.0-m.y. record of carbonate preservation from the deep Pacific [28] does show significantly poorer preservation in the late Pliocene versus the Pleistocene.

During the Pleistocene (1.6–0 m.y.), the influence of NADW in the deep Atlantic begins to be considerably reduced during glaciations. This is indicated by the more marked divergence of Site 552 and 607 $\delta^{13}C$ values in glaciations compared to interglaciations (Figs. 2b and 3b). Further, although much of the 607 $\delta^{13}C$ signal correlates to variations in $\delta^{18}O$, two interesting features are observed; first, the glacial $\delta^{13}C$ gradient between the deep North Atlantic and the deep equatorial Pacific has varied continuously over the Pleistocene; and second, deep North Atlantic $\delta^{13}C$ values were at times indistinguishable from deep equatorial Pacific values.

In Fig. 2b, 607 and 677 $\delta^{13}C$ values converge during glaciations between 1.13–1.05 m.y., 0.83–0.70 m.y., and 0.46–0.43 m.y., or at intervals of approximately 300 kyr. This modulation does not linearly correlate to amplitude variations in $\delta^{18}O$; times of lowered interocean $\delta^{13}C$ gradients are often offset from times of greater ice volume (see also $\delta^{18}O$ stack in Fig. 5b). Spectral analysis of Site 607 $\delta^{13}C$ indicates significant variance (at 85% confidence interval) concentrated around 300 kyr, while the Pacific record (Site 677) shows variance concentrated at lower frequencies, centered on 550 kyr (Fig. 4c). The fact that little variance is observed in the 250–350 kyr frequency band in the Pacific $\delta^{13}C$ record suggests that local circulation effects, rather than global variations in the oceanic ^{13}C reservoir, are causing these variations in the deep Atlantic. In addition, no obvious concentration of power is observed in the 250–350 kyr frequency band in either the Atlantic or Pacific $\delta^{18}O$ records or in the $\delta^{18}O$ stack (Figs. 4a and b) and cross-spectral analysis indicates that coherency between $\delta^{18}O$ and $\delta^{13}C$ at Site 607 declines markedly at frequencies lower than 200 kyr. Thus, while most of the Site 607 $\delta^{13}C$ signal correlates well with variations in $\delta^{18}O$, a noticeable component varies at a 250–350 kyr periodicity not strongly recorded in global ice volume.

During certain glaciations in the late Pleistocene (including stages 12, 22, and 24) deep North Atlantic (Site 607) and deep Pacific $\delta^{13}C$ values were identical (Figs. 2b and 3b). In the modern ocean, nutrient-related aging effects result in a $> 0.4‰$ $\delta^{13}C$ difference between these two re-

gions. Because it is unlikely that circulation rates in the past were so rapid as to eliminate aging-induced $\delta^{13}C$ differences between these two sites, the similarity of 677 and 607 $\delta^{13}C$ values at these times suggests three possibilities:

(1) Another source of nutrient-depleted bottom water was available in the Pacific Ocean. In this case, the Southern Ocean would be more nutrient-enriched than either the Atlantic or Pacific basins. Oppo et al. [29] show that $\delta^{13}C$ values in the Southern Ocean are more negative than Pacific deep water $\delta^{13}C$ values during glacial stages 6, 8, 10, and 12, implying that a source of nutrient-depleted water may have existed in the Pacific Ocean. This is in agreement with previous studies of the last glacial maximum which also suggested that a source of nutrient-depleted water existed in the Pacific Ocean [5 and references therein].

(2) The residence time of deep water in the Atlantic increased. Because $\delta^{13}C$ is not a conservative tracer, an increase in the residence time of water in the deep Atlantic could lower $\delta^{13}C$ values at site 607 regardless of initial source water values. At the same time, the residence time of water in the Pacific would have to decrease or remain the same.

(3) The species adjustment used to calibrate $\delta^{13}C$ values of *Uvigerina* to *Cibicidoides* (believed to accurately record the $\delta^{13}C$ of sea water ΣCO_2) is either incorrect or varies through time. In this work, 0.9‰ [16] is the correction used for $\delta^{13}C$ comparisons between site 607, where *Cibicidoides* is abundant, and site 677, where *Uvigerina* was the primary species analyzed. Alternatively, if a 0.75‰ correction [30] is used, then 677 and 607 $\delta^{13}C$ values converge but do not quite meet. A recent evaluation of paired species offsets in the Southern Ocean [29] shows that while interglacial offsets between *Uvigerina* and *Cibicidoides* are ~ 0.9‰, glacial offsets appear to be less. This observation is in agreement with Zahn et al. [31] who showed that $\delta^{13}C$ offsets between *Uvigerina* and *Cibicidoides* varied downcore. Given these uncertainties, and recognizing that the $\delta^{13}C$ records shown in Figs. 2b and 3b may not always accurately reflect seawater $\delta^{13}C$ values, we have elected to use the widely accepted species corrections outlined by Shackleton and Hall [16].

Any combination of the above effects could explain the apparent absence of a $\delta^{13}C$ gradient between the eastern equatorial Pacific and the North Atlantic. Taken at face value, the convergence of Atlantic and Pacific $\delta^{13}C$ values in stages 12, 22, and 24 implies that a fundamentally different pattern of circulation existed at these times (and probably during the other glacial episodes when 607 and 677 $\delta^{13}C$ values converge significantly but do not meet). From the extremely large amplitude (> 1.5‰) of the $\delta^{13}C$ signal at Site 607 it seems clear, however, that the major (if not the largest) circulation changes were taking place in the Atlantic basin. It is on these variations that we now focus.

3.3. Calibration of Atlantic–Pacific $\delta^{13}C$ gradients

In an attempt to isolate the $\delta^{13}C$ component at Site 607 that is attributable to circulation changes from that caused by global ocean $\delta^{13}C$ changes which affect all records (and to better depict visually the relative strength of NADW production over the last 2.5 m.y.), we have calculated an Atlantic–Pacific fractionation index using the following equation [after 14]:

$$\%\ \text{ATLANTIC vs. PACIFIC} = \left(\delta^{13}C_{S607} - \delta^{13}C_{S677}\right)/\left(\delta^{13}C_{S552} - \delta^{13}C_{S677}\right) \times 100\%$$

Essentially, this is a percent measure of where 607 $\delta^{13}C$ values fall relative to the two $\delta^{13}C$ endmembers at any one time. For instance, if a 607 $\delta^{13}C$ value falls exactly intermediate to 552 and 677 values then %ATL/PAC would be 50%; if the 607 value equalled the 677 (Pacific) value, then %ATL/PAC would be 0%, and so forth. High %ATL/PAC values suggest that NADW formation is relatively strong while low values suggest that very little NADW is making it to the deep North Atlantic.

Before calculation of %ATL/PAC, all three isotope records, 552, 607, and 677, were interpolated to a 3.4-kyr sample spacing. Gaps in the %ATL/PAC proxy (Fig. 5d) represent intervals of unrecovered or disturbed sediment at Site 552. Because this calculation looks only at the *relative* $\delta^{13}C$ changes between Site 607 and the other two sites, we can rule out the possibility that this proxy is recording either global changes in the oceanic $\delta^{13}C$ reservoir or changes in surface pre-

formed nutrient contents at the site of NADW formation.

In addition, because we lack a long high-resolution record from the Southern Ocean, the effect of circulation changes originating in the Antarctic region are uncertain. At times when the Southern Ocean was more nutrient-enriched than the Pacific Ocean, the %ATL/PAC index would underestimate the relative strength of NADW production (and vice-versa). If the 0.7-m.y. long Southern Ocean record of Oppo et al. [29] is used instead of site 677, changes of 5–15% in the %ATL/PAC index are observed during glaciations in the Brunhes. Much smaller changes are observed during interglaciations. (This is because $\delta^{13}C$ values at Sites 552 and 607 are much more similar during interglaciations and, thus, the %ATL/PAC index is relatively insensitive to $\delta^{13}C$ differences between the Southern Ocean and Pacific at these times.) The overall pattern of variation in %ATL/PAC does not change when the Southern Ocean record of Oppo et al. [29] is used.

Figure 5d shows that from 2.5 to 1.6 m.y. %ATL/PAC at Site 607 was relatively high during glacial episodes, with the proportion of northern component water always greater than at 18 kyr. The small $\delta^{13}C$ gradients between Sites 552 and 607 suggest that NADW production was relatively strong through this interval. If ice sheet size is a major factor controlling cooling of the North Atlantic [32], then less suppressed glacial NADW is in accordance with the smaller $\delta^{18}O$ amplitudes and the smaller amounts of ice-rafted detritus that are observed in the mid-latitude North Atlantic at this time [15,20]. Two episodes of lower than average %ATL/PAC, around 2.40 and 2.05 Ma, correspond to times of greater $\delta^{18}O$ values (Fig. 5b) and an interval of high %ATL/PAC between 2.35 and 2.20 Ma is characterized by relatively smaller ice volumes. Thus, in the late Pliocene, the magnitude of NADW suppression during glaciations is generally well-correlated to overall trends in ice volume.

The first episodes of severe glacial NADW reduction (greater than 50%) that we can infer from Fig. 5d fall at 1.13 and 1.03 Ma (stages 38 and 34). Large reductions in the influence of NADW also occur between 0.83 and 0.70 Ma (glacial stages 24–18) and at 0.44 Ma (stage 12). During stages 24, 22, and 12, the Atlantic Ocean at 3427 m depth (41° N, 33° W) was bathed by a water mass indistinguishable in nutrient content from that observed in the deep Pacific. A $\delta^{13}C$ gradient of approximately 1.0‰, sharper than any observed in the deep ocean today, existed between 42° N at 3427 m and 56° N at 2301 m in the North Atlantic.

The amplitude mismatch, at long wavelengths, between changes in deep ocean circulation and ice volume is especially obvious for the last five glacial cycles (see Figs. 3 and 5). Stages 12 and 10 are characterized by slightly smaller global ice volumes in our $\delta^{18}O$ stack, yet the calculated reduction in NADW influence is stronger than for stages 6 and 2. Over the last 400 kyr, the relative suppression of NADW appears to have become less severe, with the fraction of glacial NADW generally increasing toward the present.

This decline in the influence of corrosive low-$\delta^{13}C$ water of southern origin would imply that glacial $CaCO_3$ preservation should be increasing in the North Atlantic over the last 400 kyr. Crowley [33], using various dissolution indicators, demonstrated that this was true and pointed out that the relationship between dissolution and ice volume was not linear. Droxler et al. [34] showed a similar dissolution trend for glacial intervals using percent aragonite content of cores from the Bahama Banks, while Haddad [35] demonstrated that pteropods abundances in the Atlantic also reflect decreasing dissolution in glacial intervals since stage 10.

Less clear-cut is the relationship between relative NADW strength shown here and the longer dissolution records of Droxler et al. [34] and Farrell and Prell [28]. Cyclic variations in these records (not including primary Milankovitch bands at 96, 41, and 23 kyr) appear to be at longer periods (> 400 kyr) than are observed at site 607. These variations, possibly reflecting transfers between global carbon reservoirs, may be related to the long-wavelength cyclicity (centered on 550 kyr) observed in the spectra of the site 677 $\delta^{13}C$ record.

The subtle decoupling of ice volume and ocean circulation is relevant to hypotheses which explain glacial reduction in NADW production. Results from atmospheric general circulation models [32] show that the North American ice sheet, by far the single greatest contributor to the global ice-volume signal [22], directly controls North Atlantic sur-

face-ocean temperatures via strong cold winds that are generated on the northern ice-sheet flanks and blow out across the ocean. (This linkage was independently inferred from the strong correlation of $\delta^{18}O$ and sea-surface temperature (SST) records from the high-latitude North Atlantic at the 100 and 41 kyr frequencies in the late Pleistocene [36].) Lower sea-surface temperatures and expansion of sea ice in the North Atlantic then contribute to the suppression of NADW formation [e.g. 30,37]. This link was confirmed by Boyle and Keigwin [38] who showed that reductions in NADW formation, during the last glacial maxima and the Wisconsin–Holocene deglaciation, were associated with reductions of sea-surface temperatures in the North Atlantic. Thus, we might expect relatively greater reductions in the influence of NADW at times of greater ice volume and lowered North Atlantic SST.

Although site 607 is located south of the latitude of strongest $\delta^{18}O$/SST linkage (50–55° N; Site 607 is at 41° N), we compared faunal records of SST and %ATL/PAC to see if a better correlation was observed between deep circulation and SST at long wavelengths (> 100 kyr) than was observed for $\delta^{18}O$. In the North Atlantic at Site 607, SST (Fig. 5c; [21]) correlates equally well with Site 607 $\delta^{18}O$, as with Site 607 $\delta^{13}C$, and %ATL/PAC ($r_{O18} = 0.56$, $r_{C13} = 0.54$, $r_{NADW} = 0.53$). A general trend toward colder sea-surface temperatures observed between 0.9 and 0.7 m.y. correlates with greatly reduced Atlantic–Pacific $\delta^{13}C$ gradients; however, over the last 400 kyr, SST and $\delta^{18}O$ values seem better correlated, with no obvious long-wavelength trend in glacial SST values.

Between 1.25 and 1.00 Ma, long-wavelength trends in SST and the %ATL/PAC index appear to be almost out of phase. However, this may be related to the influence, from further north, of an unusually warm no-analog fauna which characterized this time interval (documented by Ruddiman et al. [21] at sites from 50° N and 56° N). Overall, the record of SST, like $\delta^{18}O$, exhibits a long-wavelength amplitude mismatch with the record of NADW circulation. The SST–deep water circulation linkage appears to be very strong on glacial–interglacial time scales. However, this linkage is more complex when variations on > 200 kyr time scales are considered.

4. Discussion

While the general pattern of reduced NADW formation during times of ice growth suggests that ice sheet forcing is probably the major influence controlling glacial to interglacial variations in deep water circulation, these data demonstrate that not all glaciations are alike. The apparent influence of Southern Ocean/Pacific water in the North Atlantic at 440 kyr BP was almost twice what it was during the last glacial maximum, yet the amplitudes of the $\delta^{18}O$ signal at these times are almost identical. Similarly, although the fine details of Fig. 5d are suspect due to vagaries in sampling, large-scale trends in glacial Atlantic/Pacific $\delta^{13}C$ gradients appear to exhibit a long-term (300 kyr) pseudo-periodicity not observed in the ice-volume record. Seemingly originating in the North Atlantic, this long wave-length variation in glacial deep-water circulation cannot be explained by variations in global ice volume, unless scenarios are invoked whereby increased ice volume in North America is masked by reductions almost everywhere else.

We can also rule out the possibility that the cyclic glacial $\delta^{13}C$ variations observed at Site 607 are due to global transfers between carbon reservoirs. This effect would be factored out by the calculation of %ATL/PAC in Fig. 5. Thus, while such changes contribute part of the glacial–interglacial $\delta^{13}C$ amplitude at Site 607, they cannot explain the differences in %ATL/PAC between glaciations.

Orbital variations cannot explain the 250–350 kyr cyclicity observed in Figs. 4 and 5; no primary or secondary insolation forcing exists within this frequency band [39]. The nearest eccentricity terms are at 412 and 136 kyr and no primary precession or obliquity variations are greater than 60 kyr. Combination tones arising from the interaction of primary Milankovitch frequencies can also be ruled out; for the 19, 23, 41, 96, 124, and 412 kyr periods no combination or difference tone falls between 206 and 425 kyr. In addition, it would be difficult to explain why such a beat frequency would characterize the $\delta^{13}C$ but not the $\delta^{18}O$ record, given their similarities at other frequency bands.

Many factors have been proposed to influence the formation rate of NADW. However, identify-

ing one as causal will prove difficult. GCM results show that the North American ice sheet has a major influence on the trajectory of atmospheric winds in the North Hemisphere during glaciations [32]. Thus, changes in the center of mass of an ice sheet could influence temperatures and wind patterns over the North Atlantic [21]. The trajectory of the Gulf Stream, believed to be controlled by both topography and the zero curl of the wind stress [40], may be critical. Variations in the extent of sea ice cover over the Norwegian or Labrador Seas [37], changes in the flux of MOW which contributes salt to NADW [41], or variations in the extent of evaporative transport over the Panamanian Isthmus (which would also affect the salt transport to the North Atlantic [42]) could all potentially modify the flux of North Atlantic deep water.

Similarly, Arctic Ocean salinity and ice cover, controlled by continental drainage and fresh water inputs from the Baltic and North Seas [43], may vary independently of continental ice volume. Recent general circulation model results [44] suggest that variations in Arctic sea ice limits could have a significant impact on North Atlantic sea-surface temperatures and salinity, while having little effect on summer temperatures over North America and Europe, areas of land ice accumulation.

Tracing the source of the circulation forcing will require the collection of high-resolution climate records from many areas. Yet, even if we can trace these deep-water variations to their source, we must still ask what is causing this forcing to vary at a quasi-periodicity not found in ice sheets or orbital signals. Are the underlying causes tectonic in origin [45–47]? Or are they stochastic in origin [e.g. 48,49], perhaps driven by variations in atmospheric or ocean temperatures which influence sea ice and deep water production but are not large enough to affect continental ice volumes.

Whatever the cause, the glacial variations in deep Atlantic circulation bring into question the role of such changes in controlling atmospheric ρCO_2 and climate. The vertical redistribution of nutrients, observed in the Atlantic Ocean for the last glaciation [14,38], has been proposed as a cause of the G–I CO_2 changes observed in ice cores [2]. Part of this redistribution may be due to the conversion of NADW to intermediate waters, but Boyle [2] proposes that relatively small CO_2 changes (~ 10 ppm) result from this mechanism. Broecker and Peng [4], by contrast, have emphasized the importance of NADW formation in controlling glacial to interglacial changes in atmospheric ρCO_2. They propose that an increase in the alkalinity of Antarctic surface waters during the Wisconsin glaciation caused the decreased CO_2 levels observed in air trapped in polar ice cores. This rise in polar surface water alkalinity is a direct consequence of decreased NADW formation during glacial times.

However, over the last 160 kyr, the Vostok CO_2 record [50] shows a much higher correlation to $\delta^{18}O$ (ice volume) records than to $\delta^{13}C$ (circulation) records from the deep Atlantic. This would seemingly support Boyle's contention that changes in NADW flux would have a relatively small impact on atmospheric ρCO_2 values (the implied assumption being that such circulation-induced CO_2 changes would then affect ice volume). Likewise, the fact that our %ATL/PAC index does not linearly correspond to variations in $\delta^{18}O$ (e.g. stage 12 versus last glacial maximum) also suggests that NADW variations may not be major influence on atmospheric ρCO_2 levels. Alternatively, if NADW suppression is a major cause of lower glacial ρCO_2 values, as proposed by Broecker and Peng [4], then global ice volume may be relatively insensitive to atmospheric CO_2 variations.

Lastly, Broecker et al. [51] and Manabe and Stouffer [52] have proposed that the ocean has two stable states; one in which NADW formation is strong and one in which it is weak. These two stable modes correspond to interglacial and glacial times, respectively. While the Atlantic–Pacific $\delta^{13}C$ gradients indicate that NADW production is always relatively weaker during glacials, just how weak it is cannot be predicted. A continuum of glacial deep water states is observed over the last 2.5 m.y., implying that deep water circulation variations do not occur bimodally.

5. Conclusions

(1) As during the most recent glaciation, the presence of nutrient-enriched, low $\delta^{13}C$ water in the deep Atlantic Ocean at times of increased ice volumes is observed throughout the last 2.5 m.y.

with $\delta^{13}C$ and $\delta^{18}O$ in phase to within 2 kyr. Significant decreases in the production of glacial NADW appear to have begun after 1.5 Ma, earlier than the transition to larger ice sheets observed between 0.9 and 0.4 m.y. [17,25].

(2) At a number of times since 1.1 Ma, $\delta^{13}C$ values at Site 607 are indistinguishable from equatorial Pacific values (Site 677), indicating that water masses with similar nutrient contents occupied the deeper sections of both oceans. This suggests that NADW production was severely limited and that a source of nutrient-depleted deep water may have existed in the Pacific Ocean at these times. The deep ocean appeared to be exceptionally enriched in nutrients, with sharp $\delta^{13}C$ gradients between 42° N (3427 m) and 56° N (2301 m) in the Atlantic Ocean.

(3) Glacial reduction of NADW appears to have been especially severe between 1.13–1.05 Ma, 0.83–0.70 Ma and 0.46–0.43 Ma. This modulation, at an approximate frequency of 300 kyr, is not observed in $\delta^{18}O$ records and, hence, export of NADW relative to inflow from the Southern Ocean/Pacific does not vary linearly with ice volume. This subtle decoupling of ice volume and deep Atlantic $\delta^{13}C$ indicates that another climate forcing factor must exist on 10^5–10^6 year time scales. The modulation of NADW strength also suggests that, rather than two stable modes, the ocean exhibits a continuum of circulation states.

(4) The amplitude of the glacial–interglacial $\delta^{13}C$ signal appears to have been anomalously small at Sites 677 and 552 over the last 125 kyr, relative to much of the Plio–Pleistocene. Possibly the global reservoir component of the G–I $\delta^{13}C$ signal was greater in the past, and/or significantly larger variations in $\delta^{13}C$ due to circulation changes occurred in the intermediate depth North Atlantic (Site 552) and deep equatorial Pacific (Site 677) over much of the late Pliocene and Pleistocene.

(5) The average Atlantic/Pacific $\delta^{13}C$ gradient appears to have decreased slightly (by ~ 0.2‰) over the last 2.5 m.y. indicating that the average nutrient content of the world's oceans may have decreased. In conjunction with such decrease, the mean ocean $\delta^{13}C$ value (best represented by site 677 in the deep equatorial Pacific) appears to have increased by ~ 0.5‰.

Acknowledgements

We are grateful to Ann Esmay for technical assistance and to W.S. Broecker, W. Curry, and J. Imbrie for helpful reviews. This research was supported by grants OCE85-21514 and OCE88-10949 from the Ocean Sciences Section of the National Science Foundation. This is Lamont-Doherty Geological Observatory contribution no. 4581.

References

1 L.V. Worthington, The Norwegian Sea as a Mediterranean basin, Deep Sea Res. 17, 77–84, 1970.
2 E.A. Boyle, The role of vertical chemical fractionation in controlling late Quaternary atmospheric carbon dioxide, J. Geophys. Res. 93, 15701–15714, 1988.
3 R.S. Keir, On the late Pleistocene ocean geochemistry and circulation, Paleoceanogr. 3, 413–445, 1988.
4 W.S. Broecker and T.-H. Peng, The cause of the glacial to interglacial atmospheric CO_2 change: A polar alkalinity hypothesis, Global Biogeochem. Cycles, 1989 (in press).
5 W.B. Curry, J.C. Duplessy, L.D. Labeyrie, and N.J. Shackleton, Quaternary deep-water circulation changes in the distribution of $\delta^{13}C$ of deep water ΣCO_2 between the last glaciation and the Holocene, Paleoceanogr. 3, 317–342, 1988.
6 P.M. Kroopnick, The distribution of ^{13}C of ΣCO_2 in the world oceans, Deep Sea Res. 32, 57–84, 1985.
7 W.S. Broecker, A revised estimate for the radiocarbon age of North Atlantic Deep Water, J. Geophys. Res. 84, 3218–3226, 1979.
8 N.J. Shackleton, Tropical rainforest history and the equatorial Pacific carbonate dissolution cycles, in: Fate of Fossil Fuel CO_2 in the Oceans, N.R. Andersen and A. Malahoff, eds., pp. 401–427, Plenum, New York, N.Y., 1977.
9 H. Craig, Carbon-13 in plants and the relationships between carbon-13 and carbon-14 variations in nature, Geology 62, 115–149, 1953.
10 J.C. Duplessy, N.J. Shackleton, R.G. Fairbanks, L. Labeyrie, D. Oppo, and N. Kallel, Deep water source variations during the last climatic cycle and their impact on the global deepwater circulation, Paleoceanogr. 3, 343–360, 1988.
11 E.A. Boyle and L.D. Keigwin, Comparison of Atlantic and Pacific paleochemical records for the last 215,000 years: changes in deep ocean circulation and chemical inventories, Earth Planet. Sci. Lett. 76, 135–150, 1985/86.
12 W.B. Curry and G.P. Lohmann, Reduced advection into Atlantic Ocean deep eastern basins during last glacial maximum, Nature 306, 577–580, 1983.
13 N.J. Shackleton, J. Imbrie and M. Hall, Oxygen and carbon isotope record of East Pacific core V19-30: implications for the formation of deep water in the late Pleistocene North Atlantic, Earth Planet. Sci. Lett. 65, 233–244, 1983.

14 D.W. Oppo and R.G. Fairbanks, Variability in the deep and intermediate water circulation of the Atlantic Ocean: northern hemisphere modulation of the Southern Ocean, Earth and Planet. Sci. Lett. 86, 1–15, 1987.
15 M.E. Raymo, W.F. Ruddiman, J. Backman, B.M. Clement and D.G. Martinson, Late Pliocene variation in Northern Hemisphere ice sheets and North Atlantic deep water circulation, Paleoceanogr. 4, 413–446, 1989.
16 N.J. Shackleton and M.A. Hall, Oxygen and carbon isotope stratigraphy of Deep Sea Drilling Project Hole 552A: Plio-Pleistocene glacial history, in: Initial Rep. Deep Sea Drill. Proj. 81, J. Backman, ed., pp. 599–610, U.S. Gov. Print. Off., Washington, D.C., 1984.
17 W.F. Ruddiman, M.E. Raymo, D.G. Martinson, B.M. Clement and J. Backman, Pleistocene evolution of Northern Hemisphere climate, Paleoceanogr. 4, 353–412, 1989.
18 N.J. Shackleton and M.A. Hall., Stable isotopic history of the Pleistocene at ODP Site 677, in: Proc. Ocean Drill. Program 111, K. Becker, H. Sakai et al., eds., U.S. Gov. Print. Off., Washington, D.C., in press.
19 D.G. Martinson, W. Menke and P. Stoffa, An inverse approach to signal correlation, J. Geophys. Res. 87, 4807–4818, 1982.
20 N.J. Shackleton, J. Backman, H. Zimmerman, D.V. Kent, M.A. Hall, D.G. Roberts, D. Schnitker and J. Baldauf, Oxygen isotope calibration of the onset of ice-rafting and history of glaciation in the North Atlantic region, Nature 307, 620–623, 1984.
21 W.F. Ruddiman, A. McIntyre and M. Raymo, Paleoenvironmental results from North Atlantic Sites 607 and 609, in: Initial Rep. Deep Sea Drill. Proj. 96, W.F. Ruddiman, R. Kidd et al., eds., pp. 855–878, U.S. Gov. Print. Off., Washington, D.C., 1986.
22 A.C. Mix, The oxygen-isotope record of glaciation, in: North America and adjacent oceans during the last deglaciation, W.F. Ruddiman and H.E. Wright, eds., pp. 111–136, Geol. Soc. Am., 1987.
23 W.B. Curry and K. Miller, Oxygen and carbon isotopic variation in Pliocene benthic foraminifera of the equatorial Atlantic, in: Proc. Ocean Drill. Program 108, W.F. Ruddiman, M. Sarnthein et al., eds., U.S. Gov. Print. Off., Washington, D.C., in press.
24 A. Berger, Long-term variations of caloric insolation resulting from the earth's orbital elements, Quat. Res. 9, 139–167, 1978.
25 W.L. Prell, Oxygen and carbon isotopic stratigraphy for the Quaternary of Hole 502B: evidence for two modes of isotopic variability, in: Initial Rep. Deep Sea Drill. Proj. 68, W.L. Prell, J.V. Gardner et al., eds., pp. 455–464, U.S. Gov. Print. Off., Washington, D.C., 1982.
26 J. Imbrie, J.D. Hays, D.G. Martinson, A. McIntyre, A.C. Mix, J.J. Morley, N.G. Pisias, W.L. Prell and N.J. Shackleton, The orbital theory of Pleistocene climate: support from a revised chronology of the marine $\delta^{18}O$ record, in: Milankovitch and Climate, Part 1, A. Berger et al., eds., pp. 269–305, Reidel, Dordrecht, 1984.
27 E.A. Boyle, Paired carbon isotope and cadmium data from benthic foraminifera: Implications for changes in oceanic phosphorus, oceanic circulation, and atmospheric carbon dioxide, Geochim. Cosmochim. Acta 50, 265–276, 1986.
28 J. Farrell and W. Prell, manuscript in preparation.
29 D.W. Oppo, R.G. Fairbanks, and A. Gordon, Late Pleistocene Southern Ocean $\delta^{13}C$ variability: North Atlantic deep water modulation of atmospheric CO_2, Paleoceanogr. (submitted).
30 A.C. Mix and R.G. Fairbanks, North Atlantic surface-ocean control of Pleistocene deep-ocean circulation, Earth Planet. Sci. Lett. 73, 231–243, 1985.
31 R. Zahn, K. Winn, and M. Sarnthein, Benthic foraminiferal $\delta^{13}C$ and accumulation rates of organic carbon: *Uvigerina perigrina* group and *Cibicidoides wuellerstorfi*, Paleoceanogr. 1, 27–42, 1986.
32 S. Manabe and A.J. Broccoli, The influence of continental ice sheets on the climate of an ice age, J. Geophys. Res. 90, 2167–2190, 1985.
33 T.J. Crowley, Late Quaternary carbonate changes in the North Atlantic and Atlantic/Pacific comparisons, in: The Carbon Cycle and Atmospheric CO_2: Natural Variations Archean to Present, AGU Geophys. Mon. Ser. 32, 271–284, 1985.
34 A. Droxler, C.H. Bruce, W.W. Sager and D.H. Watkins, Pliocene–Pleistocene variations in aragonite content and planktonic oxygen-isotope record in Bahamian periplatform ooze, Hole 663A, in: Proc. Ocean Drill. Program 101, J.A. Austin, W. Schlager et al., eds., pp. 221–244, U.S. Gov. Print. Off., Washington, D.C., 1988.
35 G.A. Haddad, A study of carbonate dissolution, stable isotope chemistry and minor element composition of pteropods and forams deposited in the Northwest Providence Channel, Bahamas, during the past 500,000 years, M.S. thesis, Duke Univ., Durham, 1986.
36 W.F. Ruddiman and A. McIntyre, Ice-age thermal response and climatic role of the surface Atlantic Ocean, 40 °N to 63 °N, Geol. Soc. Am., Bull. 95, 381–396, 1984.
37 T.B. Kellogg, Paleoclimatology and paleoceanography of the Norwegian and Greenland Seas: glacial–interglacial contrasts, Boreas 9, 115–137, 1980.
38 E. Boyle and L.D. Keigwin, North Atlantic thermohaline circulation during the last 20,000 years linked to high latitude surface temperature, Nature 330, 35–40, 1987.
39 A. Berger, Support for the astronomical theory of climate change, Nature 269, 44–45, 1977.
40 N.P. Fofonoff, The Gulf Stream system, in: Evolution of Physical Oceanography, B.A. Warren and C. Wunsch, eds., pp. 112–139, MIT Press, Cambridge, Mass. 1981.
41 J.L. Reid, On the contribution of the Mediterranean outflow to the Norwegian–Greenland Sea, Deep-Sea Res. 26, 1199–1223, 1979.
42 W.S. Broecker, Abrupt changes in climate; past and future, EOS, Trans. Am. Geophys. Union 68, 1209, 1987.
43 K. Aagaard, J.H. Swift and E.C. Carmack, Thermohaline circulation in the Arctic mediterranean seas, J. Geophys. Res. 90, 4833–4846.
44 M.E. Raymo, D. Rind and W.F. Ruddiman, Climatic effects of reduced Arctic sea ice limits in the GISS-II GCM, Paleoceanogr. 1989 (submitted).
45 W.F. Ruddiman and M.E. Raymo, Northern hemisphere climate regimes during the past 3 Ma: possible tectonic connections, in: The past three million years: evolution of climatic variability in the North Atlantic region, N.J.

Shackleton, R.G. West, and D.Q. Bowen, eds., pp. 227–234, University Press, Cambridge, 1988.
46 M.E. Raymo, W.F. Ruddiman and P.N. Froelich, Influence of late Cenozoic mountain building on ocean geochemical cycles, Geology 16, 649–653, 1988.
47 W.F. Ruddiman and J.E. Kutzbach, Forcing of late Cenozoic northern hemisphere climate by plateau uplift in southeast Asia and the American Southwest, J. Geophys. Res., 1989 (in press).
48 B. Saltzman, Carbon dioxide and the $\delta^{18}O$ record of late-Quaternary climatic change: a global model, Clim. Dyn. 1, 77–85, 1987.
49 B. Saltzman and K.A. Maasch, Carbon cycle instability as a cause of the late Pleistocene ice age oscillations: modeling the asymmetric response, Global Biogeochem. Cycles 2, 177–185, 1988.
50 J.M. Barnola, D. Reynaud, Y.S. Korotkevich and C. Lorius, Vostok ice core provides 160,000-year record of atmospheric CO_2, Nature 329, 408–414, 1987.
51 W.S. Broecker, D.M. Peteet and D. Rind, Does the ocean–atmosphere system have more than one stable mode of operation? Nature 315, 21–26, 1985.
52 S. Manabe and R.J. Stouffer, Two stable equilibria of a coupled ocean–atmosphere model, J. Clim. 1, 841–866, 1988.